P045

Numerical Modeling for Q-anisotropy in Fractured Media

V. Roganov* (Ukrainian State Geological Research Institute), Y. Roganov (Ukrainian State Geological Research Institute) & T. Chichinina (Mexican Institute of Petroleum)

SUMMARY

A method for numerical modelling of three-component (3C) three-dimensional (3D) wavefields in horizontally layered attenuative medium is derived. The method is based on delta-operators, six-dimensional Stroh formalism and Haskell-Thomson matrix method. The earth model consists of several multi-fractured layers, each of which represented by anisotropic medium model with attenuation. The attenuative fractured medium model is described by Schoenberg's linear slip formalism developed further more by introduction of the complex-valued weaknesses in the stiffness matrix. The numerical modelling method is validated for simplified earth model, which is attenuative HTI medium due to single fracture set. The Q-anisotropy and velocity anisotropy revealed from simulated wavefiedls fairly match theory-predicted quantities.

Introduction

In this paper we propose a method for calculating seismograms for horizontally layered fractured medium with account for wave attenuation. Unlike the usual case of attenuative isotropic medium where Q-factor is a constant, we deal with the case of anisotropy of attenuation resulting in the variation of the signal waveform and spectral composition as a function of azimuth.

Method for the wave field modeling for a fractured medium with attenuation is based on the generation of the propagator matrix for a layered sequence using the six-dimensional formalism of Stroh (1962). To eliminate the instability associated with the calculation of the minors of the ill-conditioned matrices, the Δ-operator technique is used, adapted to the six-dimensional matrices (Roganov et al., 2009). The wave field is modeled by summation of the reflected or refracted plane waves by their horizontal slownesses and frequencies.

Fractured medium is described by the linear slip model developed by M. Schonberg and his colleagues (Schoenberg and Douma, 1988; Hood and Schoenberg, 1989; Schoenberg and Muir, 1989; Schoenberg and Sayers, 1995). To take into account wave attenuation caused by the friction between rough crack surfaces as well as viscous fluid flow in the cracks, Chichinina et al. (2004) develop the theory of attenuative linear slip model by introducing complex-valued weaknesses Δ_N and Δ_T. Introduction of the complex parameters Δ_N and Δ_T leads to the emergence of the phenomenon of Q-anisotropy (or anisotropy of attenuation). The properties of the anisotropic Q-factor are studied in detail by Chichinina et al. (2006, 2009). The authors of this paper show that the presence of Q-anisotropy provides additional information on the fracture orientation and fluid saturation. Chichinina et al. (2009) present the results of physical modeling of wave fields in an ultrasonic experiment and obtain the estimates of Q-factor and velocity values. The authors compare these data to the theoretical results. General properties of Q-anisotropy and Thomson style parameters for TI and orthorhombic media are presented by Zhu and Tsvankin (2006, 2007).

Taking into account the prospects of further development of this topic and its application for solving inverse problems using real data, there is a need for development of numerical wavefield simulation based on the linear slip model with attenuation. In this paper, the Haskell-Thomson method (Thomson, 1950; Haskell, 1953) of wavefield modeling has been generalized for the linear slip model with attenuation. This method is used for simulation of *qP*-wavefield with the model-input parameters estimated by Chichinina e*t al.* (2009) from physical modeling. From the simulated wavefield data, the *qP*-wave attenuation is estimated as a function of wave propagation angle, using spectral ratio method. The group velocities are determined using travel times. Comparison of the obtained relationships to the theoretical ones illustrates the correctness of the wavefield modeling.

Theory

Wavefield generation for a stack of anisotropic layers using the Haskell-Thomson method and Δ-operator technique is described in detail by Roganov e*t al*. (2009). In this way we will only introduce the necessary denotations and give more detailed description of the generation of elasticity matrices for the attenuative linear slip model (Schoenberg and Muir, 1989, Chichinina e*t al.*, 2006).

Let's consider a medium consisting of n plane horizontal layers with the thicknesses h_i $(i=1,\ldots,n)$ bounded by two half-spaces (the upper, $i=0$, and the lower, $i=n+1$). Let's assume that these layers have welded contacts and contain several systems of fractures. According to the Haskell-Thomson method, the wavefields of velocities of displacement and stress $\mathbf{f}(z_1)$ and $\mathbf{f}(z_{n+1})$ at the interfaces between the half-spaces are given by the equation $\mathbf{f}(z_{n+1}) = \mathbf{P}\mathbf{f}(z_1)$, where $\mathbf{P} = \exp\{j\omega h_n \mathbf{M}^{(n)}\}\ldots\exp\{j\omega h_1 \mathbf{M}^{(1)}\}$ is the six-dimensional propagator matrix for the sequence of layers, and $\mathbf{M}^{(i)}$ are the fundamental matrices of the layers, $j=\sqrt{-1}$. The amplitude propagator **H** and the scattering matrix $\mathbf{K}=(k_{ij})_{ij=1,6}$, are derived from the matrix **P**. The matrix **K** includes the transmission and reflection coefficients of all the types of upgoing and downgoing waves, and these coefficients can be obtained from the following formulas:

$$k_{ij} = \frac{\Delta_{i456,j456}}{\Delta_{456,456}},\ k_{4j} = -\frac{\Delta_{456,j56}}{\Delta_{456,456}},\ k_{5j} = \frac{\Delta_{456,j46}}{\Delta_{456,456}},\ k_{6j} = -\frac{\Delta_{456,j45}}{\Delta_{456,456}},\ (1 \le i,j \le 3) \qquad (1)$$

where $\Delta_{i_1\ldots i_m, j_1\ldots j_m} = \det(\mathbf{H}_{ij})$ is the m–order minor of the matrix **H**. Here $1 \le i_1, j_1 \le \ldots \le i_m, j_m \le 6$, $i = i_1,\ldots,i_m$, $j = j_1,\ldots,j_m$.

The delta operator technique is applied to improve the stability of calculation of the minors in the formula (1) (Dunkin 1965; Roganov *et al*., 2009).

The fields of reflected or transmitted waves related to the type β and excited by the source of type α are generated due to summation by horizontal slownesses s_1, s_2 and circular frequency ω according to the formula:

$$\mathbf{u}_\beta(x_p, y_p, z_p, t) = \sum_{s_1, s_2, \omega} \frac{\omega A(\omega) B_\alpha(s_1, s_2) k_{\alpha\beta}}{s_{3\alpha}} \exp\left[j\omega\left(s_1 x_p + s_2 y_p + s_{3\beta} z_p - t\right)\right] \mathbf{a}_{pol}, \quad (2)$$

where $k_{\alpha\beta}$ is the reflection or transmission coefficient from the scattering matrix; $s_{3\alpha}$ is the vertical slowness of the wave of type α; $A(\omega)$ is the amplitude characteristic of the signal; $B_\alpha(s_1, s_2)$ is the characteristic of the directivity of the source of type α as a function of horizontal slownesses; $\mathbf{a}_{pol}$ is the polarization vector of the wave of type β at the receiver location.

Within the scope of the linear slip theory (Schoenberg and Douma, 1988) the effective compliance matrix $\mathbf{S}$ of a layer containing several systems of fractures characterized with the compliances $\mathbf{S}_{fi}$ and located in the medium with the compliance $\mathbf{S}_b$ is given by the formula $\mathbf{S} = \mathbf{S}_b + \sum_i \mathbf{S}_{fi}$.

Let's assume that the background medium is isotropic, and the fracture systems are rotationally invariant and given by the weaknesses Δ_{Ni} and Δ_{Ti} and the normals $\mathbf{n}_i$. In this case $\mathbf{S}_{fi} = \mathbf{N}_i^T \operatorname{diag}(0,0,k_{Ni},k_{Ti},k_{Ti})\mathbf{N}_i$, where $k_{Ni} = \Delta_{Ni}\left(1-\Delta_{Ni}\right)^{-1} c_{33}^{-1}$, $k_{Ti} = \Delta_{Ti}\left(1-\Delta_{Ti}\right)^{-1} c_{55}^{-1}$, and $\mathbf{N}_i$ are the Bond's matrices (Winterstein, 1990) describing the transformation of the compliance matrices at the rotation of the coordinate system converting the X_3-axis into the vector $\mathbf{n}_i$. The presence of a single fracture system orthogonal to the X_1-axis in the isotropic background with Lame's constants λ, μ leads to a HTI medium with the elasticity matrix $\mathbf{C} = \mathbf{G} \oplus \operatorname{diag}\left(\mu, \mu(1-\Delta_T), \mu(1-\Delta_T)\right)$, where $\mathbf{G} = \left(g_{ij}\right)$, $g_{ij} = g_{ji}$ $g_{11} = \pi(1-\Delta_N)$, $g_{12} = g_{13} = \lambda(1-\Delta_N)$, $g_{22} = g_{33} = \pi\left(1-r^2\Delta_N\right)$, $g_{23} = \lambda(1-r\Delta_N)$, $\pi = \lambda + 2\mu$, $r = \lambda/\pi$ (Schoenberg and Sayers, 1995).

The parameters $\Delta_N = \Delta_N^R + i\cdot\Delta_N^I$ and $\Delta_T = \Delta_T^R + i\cdot\Delta_T^I$ are complex values in presence of attenuation. That's why the elasticity matrix $\mathbf{C}$ is also complex. And even small imaginary parts Δ_N^I and Δ_T^I can result in strong attenuation anisotropy (Chichinina, 2006). We will demonstrate this point with the aid of an example given below.

In the analysis of the synthetic data, we use exact dependence of the group velocity and Q-factor from the group angle α to the axis X_1 for HTI medium with the stiffness matrix $\mathbf{C} = (c_{ij})$. The expressions for group velocity and Q-factor are given below. Let's denote $c_{11} = \pi(1-\Delta_N)/\rho$, $c_{13} = \lambda(1-\Delta_N)/\rho$, $c_{33} = \pi\left(1-r^2\Delta_N\right)/\rho$, $c_{55} = \mu(1-\Delta_N)/\rho$. We can obtain a relationship for phase V_{ph} and group V_g velocities of *qP*-wave using the method from the article of Schoenberg and Daley (2003) with slightly corrected designations:

$$V_{ph}^2 = \frac{c_{55}}{2g} f, \quad (3)$$

где $f = 1 + eu + \gamma + \sqrt{(1+eu+\gamma)^2 - E\left(1-u^2\right)}$, $\gamma = \dfrac{2c_{55}}{c_{11}+c_{33}}$, $e = \dfrac{c_{11}-c_{33}}{c_{11}+c_{33}}$, $E = \dfrac{4\left[(c_{11}-c_{55})(c_{33}-c_{55}) - (c_{13}+c_{55})^2\right]}{(c_{11}+c_{33})^2}$,

$u = \cos 2\varphi$, φ is the phase angle from the X_1 axis in vertical plane. Let's assume that $f_1 = f_u' \sin 2\varphi / f$. The equations (5), (6) from the article of Schoenberg and Daley (2003) imply the following equations:

$$tg(\varphi - \alpha) = \operatorname{Re} f_1, \quad (4)$$

$$V_g = V_{ph}\sqrt{1+f_1^2}, \quad (5)$$

$$Q = \operatorname{Im} V_{ph}^2 / \operatorname{Re} V_{ph}^2. \quad (6)$$

In this formulas α is the group angle, and Q is the quality factor. For comparison we will also use the formula (8) from the article of Chichinina *et al.* (2009). The formula relates Q factor and the phase angle φ in the following way:

$$Q_W(\varphi) = \frac{1-\Delta_N^R\left[1-2g\sin^2\varphi\right]^2 - \Delta_T^R g \sin^2 2\varphi}{\Delta_N^I\left[1-2g\sin^2\varphi\right]^2 + \Delta_T^I g \sin^2 2\varphi}. \quad (7)$$

Numerical example

The method described above is applied for calculation of two seismograms containing radial (R) component of the direct *qP*-wave propagating in attenuative HTI medium due to single fracture set normal to *X*-axis (Fig.1). The model-input parameters are given in Table 1, where V_{P0}, V_{S0} and ρ are *P*- and *S*- wave velocities and density of the background material (Plexiglas). These parameters were estimated by Chichinina *et al.* (2009) in the laboratory ultrasonic experiment (the case of the model "Dry fractures" with the loading pressure of 4 MPa).

Table 1

V_{P0} (m/s)	V_{S0} (m/s)	ρ (kg/m^3)	Δ_N^R	Δ_N^I	Δ_T^R	Δ_T^I
2800	1300	1200	0.60	0.054	0.53	0.004

The receivers are located along the two lines: the horizontal and the vertical ones (Fig.1). The lines are located at the distance of 1 km from the source and cover the offsets from 0 to 3 km.

The formula (5) is used to calculate the dependence of group angle α from the phase angle φ for the *qP*-wave velocity (Fig.2). The angles α significantly differ from the angles φ thus testifying to the large velocity anisotropy ($[(V_{MAX} - V_{MIN})/\overline{V}]\cdot 100\% \approx 35\%$).

Figure 3 shows the gathers for horizontal (*a*, *b*) and vertical (*c*, *d*) lines of receivers. The gathers on the left (*a*, *c*) are calculated with account for attenuation (the attenuation parameters Δ_N^I and Δ_T^I are given in Table 1), while the gathers on the right ((*b, d*) are calculated without account for attenuation ($\Delta_N^I = 0$, $\Delta_T^I = 0$).

Q-factor is estimated for each receiver-point signature using the spectral ratio method. (Figure 4(a)). The group velocity V_g is estimated from the traveltimes of the direct *qP*-wave (Figure 4(b)). The estimated values of Q and V_g (marked by blue and green symbols) are overlain on the theoretical curves calculated from the formulas (6) and (5) correspondingly (marked by black line). For comparison, the same Figure 4 also contains theory-predicted dependences of *Q*-factor from the phase angle φ (formula (7)) and the phase velocity from the phase angle (denoted by red line).

Figure 4(a) shows strong attenuation anisotropy $[(Q_{MAX} - Q_{MIN})/\overline{Q}]\cdot 100\% \approx 145\%$, which is more than 100% greater than the magnitude of velocity anisotropy. It is quite natural result, as theoretically predicted and confirmed by measurements of *Q*-anisotropy by physical modeling (Zhu et al. 2007, Chichinina e*t al.* 2009),

The results demonstrate that attenuation and velocity estimated from simulated wavefiedls fairly match the theory-predicted values. Therefore, this method of wavefield modeling developed for attenuative fractured medium is correct and can be applied for solving different problems in presence of Q-anisotropy.

Conclusions

Thus, the efficient wavefield-modeling method for attenuative fractured medium has been developed and demonstrated on a simple model example with successful results.

References

Chichinina T., Sabinin V. and Ronquillo-Jarillo G. 2004, P-wave attenuation anisotropy in fracture characterization: numerical modelling for reflection data. 74th SEG Meeting, Expanded Abstracts, 143–146.

Chichinina T., Sabinin V. and Ronquillo-Jarillo G. 2006. QVOA analysis: P-wave attenuation anisotropy for fracture characterization: *Geophysics* **71**, C37–C48.

Chichinina T., Obolentseva I., Gik L., Bobrov B. and Ronquillo-Jarillo G. 2009. Attenuation anisotropy in the linear-slip model: Interpretation of physical modeling data. *Geophysics* **74**, WB165–WB176.

Dunkin I.W. 1965. Computation of modal solutions in layered elastic media at high frequencies. *Bull. Seismol. Soc. Amer.* **55**, 335-358.

Haskell N.A. 1953. The dispersion of surface waves on multilayered media. *Bul. Seismol. Soc. Amer.,* **43**(1), 17-34.

Hood J. A. and M. Schoenberg M. 1989. Estimation of vertical fracturing from measured elastic moduli. *Journal of Geophysical Research* **94**, 15611–15618.

Roganov V., Roganov Y. and Kostiukevich A. 2009. 3D-3C seismic wave modeling in multilayered anisotropic viscoelastic media using the Haskell-Thomson method. 71th EAGE Conference, Amsterdam, 8-11 June 2009, P134.

Schoenberg M. and Douma J. 1988. Elastic wave propagation in media with parallel fractures and aligned cracks. *Geophysical Prospecting*, **36**, 571–590.

Schoenberg M. and Muir F. 1989. A calculus for finely layered anisotropic media. *Geophysics*, **54**, 581–589.

Schoenberg M. and Sayers C. M. 1995. Seismic anisotropy of fractured rock. *Geophysics*, **60**, 204–211.

Schoenberg M. and Daley T.M. 2003. qSV wavefront triplication in transversely isotropic material. 73rd SEG Meeting, Dallas, Expanded Abstracts, 137–140.

Stroh A.N. 1962. Steady state problems in anisotropic elasticity. *J.Math.Phys.* **41**. P. 77-103.

Thomson W.T. 1950. Transmission of classic waves through a stratified solid material. *J.Appl. Phys.*, **21**(1), 89-93.

Winterstein D. 1990. Velocity anisotropy terminology for geophysicist. *Geophysics* **55**, 1070-1088.

Zhu Y. and Tsvankin I. 2006. Plane-wave propagation in attenuative transversely isotropic media. *Geophysics*, **71**(2), T17-T30.

Zhu Y. and Tsvankin I. 2007. Plane-wave attenuation anisotropy in orthorhombic media. *Geophysics*, **72**(1), D9-D19.

Zhu, Y., I. Tsvankin, P. Dewangan, and K. vanWijk, 2007, Physical modeling and analysis of P-wave attenuation anisotropy in transversely isotropic media: Geophysics, **72**, no. 1, D1–D7.

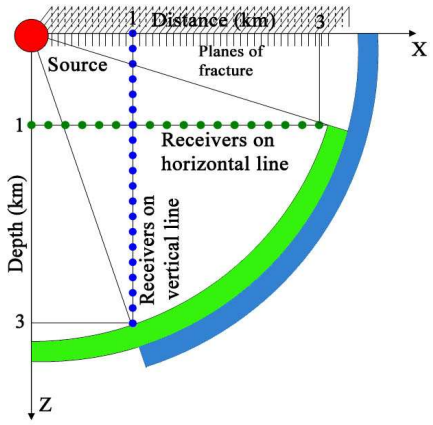

Figure 1. *Acquisition geometry. The receivers are located along the horizontal and vertical lines. Fractures are perpendicular to the X-axis.*

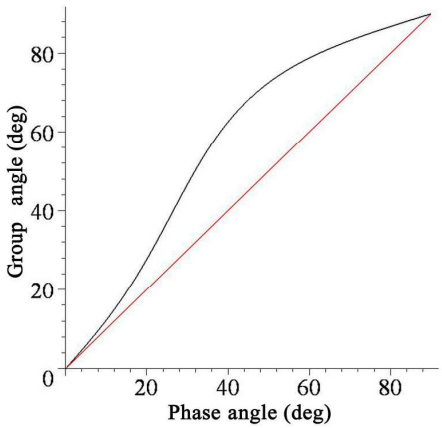

Figure 2. *Dependence of the group angle from the phase angle for qP-wave velocity (black line) is not a linear function (the latter marked by red line).*

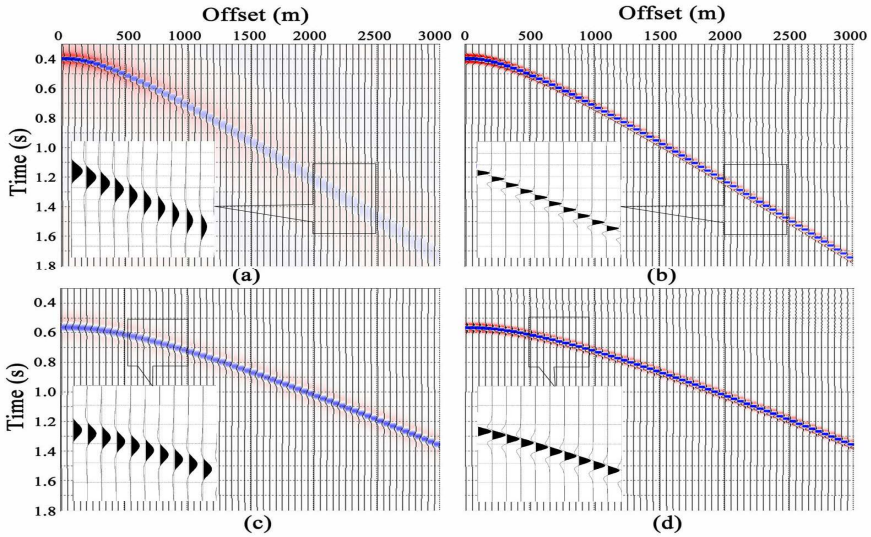

Figure 3. *Gathers for horizontal (a, b) and vertical (c, d) lines of receivers. Left images (a,c) are obtained with attenuation (see* Δ_N^I *and* Δ_T^I *in Table 1), and right images (b,d) are obtained without attenuation (* $\Delta_N^I = 0$ *and* $\Delta_T^I = 0$ *).*

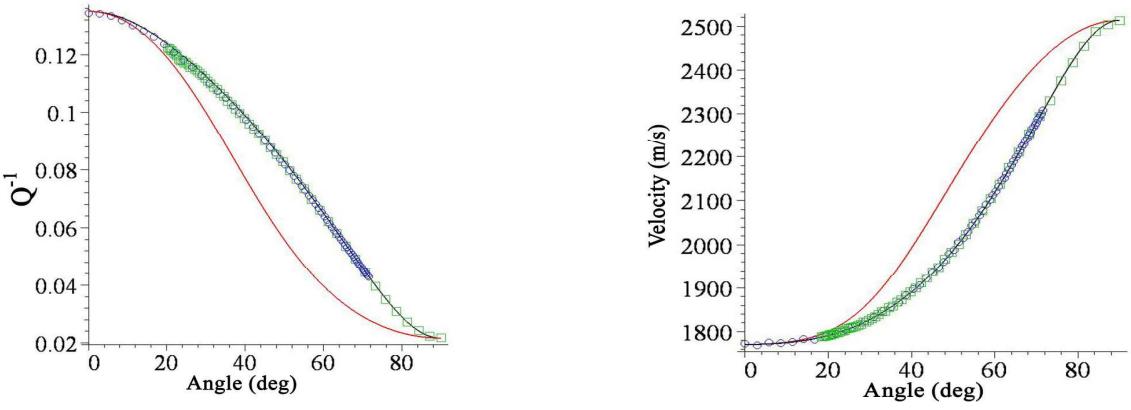

(a) *(b)*

Figure 4. *The values of* Q^{-1} *(a) and group velocities (b) for qP-wave. The values were derived from the spectra and traveltimes correspondingly. The blue circles denote receivers located along the vertical line and green squares denote receivers located along the horizontal line. The black curves represent theoretical functions, while the red curves represent weak anisotropy approximations.*